Energy-Efficient Optimal Water Flow Considering Pump Efficiency

Krishna Sandeep Ayyagari*, Shen Wang*, Nikolaos Gatsis*, Ahmad F. Taha*, and Marcio Giacomoni†

2021 IEEE Madrid PowerTech | 978-1-6654-3597-0/21/$31.00 ©2021 IEEE | DOI: 10.1109/PowerTech46648.2021.9494803

***Abstract*—The electricity demand for water supply purposes is steadily increasing due to urbanization. Therefore, water distribution networks (WDNs) are becoming energy-intensive due to the wide-spread deployment of electricity-driven water pumps. Energy-efficient operation of water pumps is a significant concern for WDN operators. To this end, this paper formulates the optimal water flow (OWF) problem to optimally schedule pumps and valves with the objective of minimizing the pump power consumption while at the same time accounting for the flow-dependent pump efficiency in WDNs. The resulting OWF problem is a mixed-integer nonlinear program (MINLP). The problem includes a fractional (nonconvex) objective and nonconvex constraints due to the WDN hydraulics, and is hard to solve. A novel successive linear approximation-based approach is used to overcome the nonconvex hydraulic constraints. Furthermore, Dinkelbach's algorithm is used to tackle the fractional pump power objective. Finally, a solver called convex optimal water flow (C-OWF) is developed, which relies on solving a sequence of mixed-integer linear programs. A case study verified by simulation software EPANET illustrates the C-OWF's benefits in operating the pump near maximum efficiency and reducing pump power compared to conventional rule-based designs.**

***Index Terms*—Water distribution networks, mixed-integer program, optimal water flow, successive approximation, fractional programming**

I. Introduction

In 2015, 54% of the world's population lived in urban areas. By 2030, the global population is expected to reach 8.5 billion, with approximately 60% expected to live in cities with urbanization trends continuing around the world [1]. Water demand in cities will consequently continue to rise in coming years. To cater to the rising water demand, the water distribution netwroks (WDNs) are becoming energy-intensive due to the wide-spread deployment of electric-driven water pumps. The energy costs for operating pumps constitute the major operating costs of water utilities. Specifically, approximately 4% of the total electricity consumption in the United States is attributed to the activities of the WDNs [2] and responsible for around 5% of national greenhouse gas emissions per annum [3].

The inefficient operation of electric-driven water pumps is largely the driving factor of high operational cost in WDNs. The largest pumping energy savings occur when pumps are correctly sized for the WDN under consideration and operated around their maximum efficiency. However, most of the pumps in existing WDNs are oversized (many of them over 20%), highlighting an excellent opportunity to address large-scale energy inefficiency [4]. See also [5], [6] for a detailed review of energy efficiency in WDNs. Furthermore, due to the advancement of smart grids, the coordinated operation of water and power distribution systems is considered the viable option to enhance security and reliability of both systems [7], [8]. In this regard, the energy-efficient operation of WDNs is critical for the joint management of water and power distribution networks as well.

The heart of any attempt to improve the energy efficiency in WDNs can be passed through actions such as (1) optimal pump scheduling, and (2) operating pumps close to their maximum efficiency. Optimal pump scheduling can be achieved by solving the optimal water flow (OWF) problem given water demand forecasts. The WDN constraints such as pipe and pump hydraulic constraints render the OWF problem a difficult mixed-integer nonlinear program (MINLP). To overcome these challenges, many research efforts have been devoted to modeling, planning, analysis, and operation of WDNs, e.g., [9]–[14]. These include nonconvex, MINLP based branch and bound methods [9], piecewise linear approximations combined with branch and bound methods [10], [11], Lagrange decomposition coupled with a simulation-based, limited discrepancy search [12], applying convex relaxation techniques to convert the nonconvex OWF problem to mixed-integer second-order cone formulation [13], [14].

The works mentioned above assume the pump efficiency to be constant while solving the OWF problem. On the other hand, the pumping energy in WDNs depends on the pump flow, pump head, and the pump efficiency [15]. The pump efficiency is in general not constant, but depends on the flow through the pump (flow-dependent). Consequently, as the pump flow changes over the day, the head and the efficiency of the pump will change, affecting the amount of energy used [16]. Therefore, operating the pump at the best efficiency point is crucial for the pump's energy-efficient operation. In this regard, some researchers have attempted to optimally schedule the pumps by considering the flow-dependent pump efficiency [17] as a large-scale MINLP problem. Moreover, considering the flow-dependent pump efficiency in the pump power render the OWF problem computationally cumbersome and, therefore, hard to solve.

Although the pump scheduling problem in WDNs has been investigated in the previously mentioned literature, technical challenges remain. Specifically, most of the previously mentioned works assume linear head loss model for pumps (e.g., [13]), constant pump efficiency (e.g., [9], [10], [12]–[14]), or a linear dependence of the pump power on water flow, which is not physically correct [11]. The present work introduces techniques to account for more accurate pump modeling, namely, the nonlinear head loss model and flow-dependent efficiency.

Our previous work on WDN operations [18]–[20] has contributed linearizations through novel monomial approximations of the WDN hydraulics. Specifically, [18] deals with the water flow problem without pump scheduling, while [20] develops state estimation methods of WDNs. Pump scheduling is investigated in [19] using a heuristic algorithm by considering flow-dependent pump efficiency without introducing integer variables for pump and valve operations. In all the previously mentioned works, constant pump efficiency has been assumed.

Leveraging the recent advancements in fractional programming [21]–[23] and novel monomial approximations of the WDN hydraulics from [18]–[20], the contributions of this paper are as

*Department of Electrical Engineering, †Department of Civil and Environmental Engineering, The University of Texas at San Antonio, TX 78249. Emails:{krishnasandeep.ayyagari, shen.wang, nikolaos.gatsis, marcio.giacomoni, ahmad.taha}@utsa.edu. This material is based upon work supported by the National Science Foundation under Grant No. 1847125.

978-1-6654-3597-0/21/$31.00 ©2021 IEEE

follows: (1) We expand our previous works [18]–[20] featuring novel monomial approximations for the WDN hydraulics to incorporate pump and valve operations in WDNs using integer variables. (2) The flow-dependent pump efficiency is explicitly accounted for in the optimization to minimize pump power. The convex optimal water flow (C-OWF) solver for solving the nonconvex OWF is developed. The C-OWF problem can be solved as a mixed-integer linear program (MILP) within reasonable computational time. It is worth emphasizing that the required number of integer variables is significantly reduced compared to approaches in the prior art. (3) The C-OWF solver's performance is accessed in terms of pump power objective improvements and energy-efficient operation compared to a rule-based design. (4) The C-OWF solver's accuracy and feasibility is demonstrated using nonlinear water flow solver EPANET [15].

The organization of the paper is given next. Section II discusses the modeling of WDNs. Section III presents the pump efficiency model. The OWF problem is formulated in Section IV as a nonlinear and nonconvex program. Section V presents the proposed approach and casts the nonconvex OWF problem into a convex OWF problem, which can be solved as a sequence of mixed-integer linear programs (MILPs). The simulation results are presented in Section VI, and the conclusions are drawn in Section VII.

II. Water Distribution Network Model

The WDN is modeled by a directed graph $(\mathcal{M}, \mathcal{L})$ where $\mathcal{M} = \{0, \ldots, M\}$ is a set of $M+1$ nodes with $\mathcal{M} = \mathcal{J} \bigcup \mathcal{R} \bigcup \mathcal{K}$, and $\mathcal{J}$, $\mathcal{R}$, and $\mathcal{K}$ respectively denote sets of junctions, reservoirs, and tanks. Let $\mathcal{L} \subseteq \mathcal{M} \times \mathcal{M}$ be the set of links connecting the nodes partitioned as $\mathcal{L} = \mathcal{P} \bigcup \mathcal{W} \bigcup \mathcal{V}$, where $\mathcal{P}$ and $\mathcal{W}$ respectively denote the sets of pumps, pipes and valves. Also, in this work, we assume that the pumps are connected to fixed-speed motors, i.e., they are fixed-speed pumps (FSPs) and has flow-dependent wire-to-water efficiency $\eta^{\text{ww}}_{ij,t} = \eta^{\text{motor}}_{ij}\ \eta^{\text{pump}}_{ij,t},\ ij \in \mathcal{P}$. In particular, the motor efficiency η^{motor}_{ij} is assumed constant [14] and pump efficiency $\eta^{\text{pump}}_{ij,t},\ ij \in \mathcal{P}$ is flow-dependent, i.e., the pump efficiency depends on the pump flow. Furthermore, the WDN operation is optimized over a horizon $\mathcal{T} = \{1, \ldots, T\}$, with δ representing the time interval between two consecutive time periods. It is worth noting that the presented optimization problem yields the directions of water flow in pipes. Next, we present the mathematical model of WDN operational constraints for $t \in \mathcal{T}$:

$$\sum_{i:ij\in\mathcal{L}} q_{ij,t} - \sum_{k:jk\in\mathcal{L}} q_{jk,t} = d_{j,t}, \quad j \in \mathcal{J} \tag{1a}$$

$$h_{i,t} - h_{j,t} = A_{ij}|q_{ij,t}|^{\mu-1} q_{ij,t}, \quad ij \in \mathcal{W} \tag{1b}$$

$$h_{k,t} = h_{k,t-1} + \frac{\delta_t}{A_k}\left(\sum_{i:ik\in\mathcal{L}} q_{ik,t} - \sum_{j:jk\in\mathcal{L}} q_{jk,t}\right), k \in \mathcal{K} \tag{1c}$$

$$h_{i,t} - h_{j,t} = \left\{ \begin{array}{l} -(h_{0,ij} - \sigma_{ij} f^{\nu}_{ij,t}),\ \text{if } x_{ij,t} = 1 \\ \text{unconstrained},\ \text{if } x_{ij,t} = 0, , ij \in \mathcal{P} \end{array} \right\} \tag{1d}$$

$$q_{ij,\min}\ x_{ij,t} \le q_{ij,t} \le q_{ij,\max}\ x_{ij,t}, \quad ij \in \mathcal{P} \tag{1e}$$

$$h_{i,t} - h_{j,t} = \left\{ \begin{array}{l} r_{ij,t},\ r_{ij,t} \ge 0,\ \text{if } v_{ij,t} = 1 \\ \text{unconstrained},\ \text{if } v_{ij,t} = 0, ij \in \mathcal{V} \end{array} \right\} \tag{1f}$$

$$q_{ij,\min}\ v_{ij,t} \le q_{ij,t} \le q_{ij,\max}\ v_{ij,t}, \quad ij \in \mathcal{V} \tag{1g}$$

$$p^{\text{pump}}_{ij,t} = \frac{\rho g}{\eta^{\text{ww}}_{ij,t}} |h_{i,t} - h_{j,t}| q_{ij,t}, \quad ij \in \mathcal{P} \tag{1h}$$

$$h_{i,t} = h^{\text{R}}_i, \quad i \in \mathcal{R} \tag{1i}$$

$$h_{j,\min} \le h_{j,t} \le h_{j,\max}, \quad j \in \mathcal{J}, \mathcal{K} \tag{1j}$$

Constraint (1a) enforces the the mass conservation at junction $j \in \mathcal{J}$ at time t, where $d_{j,t}$ is the estimated water demand at time t. Constraint (1b) formulates the head loss in pipe $ij \in \mathcal{W}$ which is approximated by the empirical Hazen-Williams equation [15], where $A_{ij} = 4.727 C_{ij}^{-1.852} \hat{d}_{ij}^{-4.871} \hat{l}_{ij}$; $\hat{d}_{ij}$ and $\hat{l}_{ij}$ are respectively the diameter and length of a circular pipe; C_{ij} is the Hazen-Williams roughness coefficient (unitless); μ is the flow exponent; and $q_{ij,t}$ is the volumetric flow rate through pipe $ij \in \mathcal{W}$. Constraint (1c) models the water tank head dynamics for tank $k \in \mathcal{K}$ with cross-sectional area A_k and initial head $h_{k,0}$ (assumed to be known).

Constraint (1d) formulates the head loss across the FSP connected between nodes i and j and is modeled according to [15, Ch. 3], where $h_{0,ij}$ is the shutoff head for the pump, σ_{ij}, ν_{ij} are the pump curve coefficients evaluated at nominal speed, $q_{ij,t}$ is the water flow through the pump and $x_{ij,t}$ is the binary variable to indicate whether the pump $ij \in \mathcal{P}$ is running at time t. Also note that the head loss of FSP $h_{ij,t}$ in (1d) is negative when the pump is on, which means that head gain is provided across the pump. The pump flow is constrained by (1e). The binary variable $x_{ij,t}$ is set to 1 when pump $(ij) \in \mathcal{P}$ is on at time t and the constraint (1d) is active; otherwise no constraint exists between $h_{i,t}$ and $h_{j,t}$. Constraints (1f) and (1g) capture the operation of pressure-reducing valves (PRVs). The binary variable $v_{ij,t}$ is set to 1 if the valve ij in $\mathcal{V}$ carries a nonzero water flow and allows nonnnegative head loss $r_{ij,t}$ from node i to node j if it is needed, i.e., $r_{ij,t} \ge 0$ [14]. When the valve carries a nonzero water flow, i.e., $v_{ij,t} = 1$, the constraints (1f) and (1g) are active; otherwise h_i, h_j are unconstrained. The FSP power consumption is captured in (1h), where ρ, g, and $\eta^{\text{ww}}_{ij,t}$ are respectively the water density, standard gravity coefficient, and pump wire-to-water efficiency. The fixed reservoir head is given by (1i) which is operational constraint and the head of the remaining nodes is constrained by (1j). Also, for simplicity let $\gamma_{ij} = \frac{\rho g}{\eta^{\text{motor}}_{ij}}, \quad ij \in \mathcal{P}$.

A more convenient mathematical formulation is needed to capture the FSP and PRV on/off status and operation logic given by (1d), (1e), (1f) and (1g). This task is accomplished using the big-*M* technique to rewrite the aforementioned constraints.

$$M(x_{ij,t} - 1) \le h_{ij,t} + [h_{0,ij} - \sigma_{ij}(q_{ij,t})^{\nu}] \tag{2a}$$

$$\le M(1 - x_{ij,t}) \tag{2b}$$

$$h_{i,t} - h_{j,t} = h_{ij,t} \tag{2c}$$

$$h_{ij,t} \le 0 \tag{2d}$$

$$x_{ij,t} \in \{0, 1\}, \quad ij \in \mathcal{P} \tag{2e}$$

Equation (2) corresponds to FSP operation, where $h_{ij,t}$ is the auxiliary variable that represents pump head loss (1d). Similarly, the PRV valve operation is modeled using the big *M* technique as follows [14]

$$-M(1 - v_{ij,t}) \le h_{ij,t} - r_{ij,t} \le M(1 - v_{ij,t}) \tag{3a}$$

$$q_{ij,\min} v_{ij,t} \le q_{ij,t} \le q_{ij,\max} v_{ij,t} \tag{3b}$$

$$0 \le r_{ij,t} \le M v_{ij,t} \tag{3c}$$

$$h_{i,t} - h_{j,t} = h_{ij,t} \tag{3d}$$

$$v_{ij,t} \in \{0, 1\}, \quad ij \in \mathcal{V} \tag{3e}$$

with auxiliary variable $h_{ij,t}, ij \in \mathcal{V}$. Next, we turn our attention to the modeling of flow-dependent pump efficiency.

III. Pump Efficiency Model

The pump efficiency is defined as the ratio of the hydraulic power produced by the pump (output) to the electric power used by the pump (input) as follows:

$$\eta^{\text{pump}}_{ij,t} = \frac{\rho g |h_{ij,t}| q_{ij,t}}{\eta^{\text{motor}}_{ij} p^{\text{pump}}_{ij,t}} \tag{4}$$

where $\rho g |h_{ij,t}| q_{ij,t}$ is the pump's hydraulic power. The constant pump efficiency model postulates that the ratio computed from (4) for

a given pump is identical for all values of the pump flow. However, pump manufacturers in practice perform experiments to determine the efficiency for different flow values by computing the pump's hydraulic power and measuring the motor's input electrical power. In general, the ratio in (4) is not constant but dependent on the pump flow.

The relationship between the fixed-speed pump's flow $q_{ij,t}$ and the pump efficiency $\eta^{\text{pump}}_{ij,t}$ can in general be described by an N-degree polynomial as follows:

$$\eta^{\text{pump}}_{ij}(q_{ij,t}, \mathbf{a}_{ij}) = \sum_{n=0}^{N} \mathrm{a}_{n,ij}(q_{ij,t})^n \tag{5}$$

where N is the degree of polynomial required to approximate the efficiency curve. The polynomial coefficients in (5) are included in vector $\mathbf{a}_{ij}$. The most most typical polynomials used in practice are of second and third degrees.

Quadratic Pump Efficiency: It is shown in [11] and [24] that for several types of pumps, the pump efficiency in (5) is approximated by the quadratic polynomial, i.e., $\mathrm{N} = 2$, and is given as

$$\eta^{\text{pump},Q}_{ij,t} = a_{0,ij} + a_{1,ij} q_{ij,t} + a_{2,ij} q^2_{ij,t} \tag{6}$$

where $\eta^{\text{pump},Q}_{ij,t}$ is the quadratic efficiency of the pump $ij \in \mathcal{P}$. The coefficients $a_{0,ij}$, $a_{1,ij}$, and $a_{2,ij}$ in (6) are approximated by the best (maximum) efficiency point of the pump (η^*_{ij}), the pump's flow at the best efficiency point (q^*_{ij}), and the origin $(0,0)$. Based on the two points $(0,0)$ and $(q^*_{ij}, \eta^*_{ij},)$, and the fact that the derivative of (6) is zero at (η^*_{ij}, q^*_{ij}), the coefficients are given as solution of the following linear system of equations:

$$a_{0,ij} = 0 \tag{7a}$$

$$a_{1,ij} q^*_{ij} + a_{2,ij} (q^*)^2_{ij} = \eta^*_{ij} \tag{7b}$$

$$a_{1,ij} + 2\ a_{2,ij} q^*_{ij} = 0 \tag{7c}$$

Equation (7a) corresponds to the point $(0,0)$; (7b) is derived from the point (q^*_{ij}, η^*_{ij}); (7c) represents the condition that $(\eta^{\text{pump},Q}_{ij,t})' \mid_{q_{ij,t}=q^*_{ij}} = 0$. Solving (7) for $a_{1,ij}$ and $a_{2,ij}$, the coefficients are $a_{1,ij} = \frac{2\eta^*_{ij}}{q^*_{ij}}$ and $a_{2,ij} = -\frac{\eta^*_{ij}}{(q^*_{ij})^2}$.

Cubic Pump Efficiency: For better accuracy in estimating the pump efficiency, a cubic polynomial is adopted in [25], i.e., $N = 3$. The polynomial is as follows:

$$\eta^{\text{pump},C}_{ij,t} = a_{0,ij} + a_{1,ij} q_{ij,t} + a_{2,ij} q^2_{ij,t} + a_{3,ij} q^3_{ij,t} \tag{8}$$

where $\eta^{\text{pump},C}_{ij,t}$ is the cubic efficiency of the pump $ij \in \mathcal{P}$. The coefficients $a_{0,ij}$, $a_{1,ij}$, $a_{2,ij}$, and $a_{3,ij}$ in (8) can be determined by three points $(0,0)$, (q^*_{ij}, η^*_{ij}), and $(\tilde{q}_{ij}, 0)$, with the additional requirement that $(\eta^{\text{pump},C}_{ij,t})' \mid_{q_{ij,t}=q^*_{ij}} = 0$. The cutoff point $(\tilde{q}_{ij}, 0)$ corresponds to the maximum flow of the pump for which the head loss across the pump is zero. Based on the knowledge of three points stated earlier and using the procedure described in [25], the cubic pump efficiency coefficients are given as follows

$$a_{0,ij} = 0 \tag{9a}$$

$$a_{1,ij} = \frac{\eta^*_{ij} q^*_{ij} \tilde{q}_{ij} (3q^*_{ij} - 2\tilde{q}_{ij})}{-(q^*_{ij})^2 (\tilde{q}_{ij} - q^*_{ij})^2} \tag{9b}$$

$$a_{2,ij} = \frac{\eta^*_{ij} (3(q^*_{ij})^2 - (\tilde{q}_{ij})^2)}{-(q^*_{ij})^2 (\tilde{q}_{ij} - q^*_{ij})^2} \tag{9c}$$

$$a_{3,ij} = \frac{\eta^*_{ij} (2q^*_{ij} - \tilde{q}_{ij})}{-(q^*_{ij})^2 (\tilde{q}_{ij} - q^*_{ij})^2} \tag{9d}$$

The coefficients for quadratic and cubic pump efficiencies computed from (7) and (9) are usually less accurate than the coefficients computed from the regression using K pairs of known flow-efficiency data points $(q_{1,ij}, \eta^{\text{pump}}_{1,ij}), (q_{2,ij}, \eta^{\text{pump}}_{2,ij}), \ldots, (q_{K,ij}, \eta^{\text{pump}}_{K,ij})$ obtained experimentally or by the pump manufacturer. When such data points are available, the following linear least squares problem can be readily solved to obtain accurate coefficients for (5), (6), or (8) [26]

$$\min_{\mathbf{a}_{ij}} \frac{1}{K} \sum_{k=1}^{K} \left[\eta^{\text{pump}}_{k,ij} - \sum_{n=0}^{N} \mathrm{a}_{n,ij} (q_{k,ij})^n \right]^2 \tag{10}$$

Note that although the present work focuses on the quadratic or cubic pump efficiencies with coefficients given by (7) and (9), our approach can still work to include (5). In addition, to prevent division by zero in the denominator of (1h) when the pump is not running, i.e., when ($x_{ij,t} = 0$ and $q_{ij,t} = 0$), we let $a_{0,ij}$ in (6) and (8) to be a small strictly positive number [11].

Finally, it is worth noting that certain pump efficiency curves reported in the literature do not go through the origin $(0,0)$, but a nonzero efficiency is given when $q_{ij} \to 0^+$; see e.g., [11, Fig. 3b] and [26, Fig. 10.16]. In this case, the coefficient $a_{0,ij}$ can be set to the corresponding value in (7a) or (9a).

IV. Optimal Water Flow Problem

In this work, the objective is to minimize the pump power consumption in WDNs:

$$\Gamma^{\text{pump}}_{ij,t}(q_{ij,t}, \eta^{ww}_{ij,t}) = p^{\text{pump}}_{ij,t}, \quad ij \in \mathcal{P} \tag{11}$$

and the objective $\Gamma^{\text{pump}}_{ij,t}(.)$ is written as

$$\Gamma^{\text{pump}}_{ij,t}(.) = \frac{\gamma_{ij} |h_{ij,t}| q_{ij,t}}{\eta^{\text{pump}}_{ij,t}} \tag{12}$$

where $\eta^{\text{pump}}_{ij,t}$ is given by (6) or (8) and $h_{ij,t}$ by (2c).

Other pertinent objectives can also be considered, such as water consumption costs, pump maintenance costs, and water delivery costs incurred by water utility operator [9], [10]. However, the pump power is typically the main contributing factor in WDN costs. Therefore, this work focuses on minimizing pump power.

The optimal water flow problem (OWF) (P1) is formulated as

$$\text{(P1)} \ \min \quad \sum_{t=1}^{T} \left[\lambda_t \sum_{ij \in \mathcal{P}} \Gamma^{\text{pump}}_{ij,t} \right] \tag{13a}$$

$$\text{over} \quad \{p^{\text{pump}}_{ij,t}, q_{ij,t}, r_{ij,t}, \eta^{\text{pump}}_{ij,t}\}^T_{t=1}, \quad \{h_{ij,t}, h_{j,t}, x_{ij,t}, v_{ij,t}\}^T_{t=1}, \quad ij \in \mathcal{L}, j \in \mathcal{M}$$

$$\text{subj. to} \quad \text{(1a)} - \text{(1c)}, \text{(1h)} - \text{(1j)}, (2), (3), (6)/(8) \tag{13b}$$

Where λ_t denotes the time-varying price.

The OWF (P1) is an MINLP. The nonconvexities stem from the head loss models of pipes and pumps (1b), (1d). Also, the objective corresponding to pump power consumption (1h) is nonconvex and computationally very expensive due to its fractional nature, i.e., the numerator and the denominator of (12) are variables. To address the above issues, we utilize novel successive linear approximations for head loss models of pipes and pumps [20], which solve a sequence of convex problems without prior knowledge of water flow directions. We tackle the fractional part of pump power in (12) using Dinkelbach's algorithm [23] and finally cast (P1) as a MILP which can be readily solved without significant computational burden. This is the theme of the following section.

V. Linear Approximations of Hydraulics and C-OWF

First, using a monomial approximation in [19], the nonlinear head loss model for pipes and pumps (1b) and (1d) are approximated by a linear form around a given point (flow value). Second, we construct an upper bound for both the numerator and the denominator of the nonconvex (fractional) FSP power consumption (1h) around a given point resulting in a linear fractional form, which enables the application of Dinkelbach's transform. The aim is to solve (P1) through a series of tractable approximating problems. We denote the value of $q_{ij,t}$ resulting from the previous approximating problem as $\langle q_{ij,t} \rangle$. The approximations are introduced next.

A. Linear Approximation of Pipe and Pump Head Loss

Using [19] and [20], we replace the nonlinear pipe and pump head loss constraint [c.f (1b) and (1d)] with their corresponding linear form as given below

$$\hat{h}_{ij,t} = \kappa_{ij,t} + q_{ij,t},\ ij \in \mathcal{W},\ t \in \mathcal{T} \tag{14a}$$

$$\hat{h}_{ij,t} = (\tau_{ij,t} + \varphi_{ij,t} q_{ij,t}),\ ij \in \mathcal{P},\ t \in \mathcal{T} \tag{14b}$$

Constraint (14a) represents the linear head loss approximation for the nonlinear pipe head loss constraint (1b), where $\kappa_{ij,t} = \langle q_{ij,t}\rangle(A_{ij}|\langle q_{ij,t}\rangle|^{\mu^{-1}}-1)$. Similarly, constraint (14b) describes the linear head loss approximation for (1d), with constants $\tau_{ij,t} = -h_{0,ij}$ and $\varphi_{ij,t} = \sigma_{ij}\langle q_{ij,t}\rangle^{\nu_{ij}-1}$. It should be noted that $\kappa_{ij,t}$ and $\varphi_{ij,t}$ are approximated using the flow value $\langle q_{ij,t}\rangle$ through pipes and pumps of the previous iteration. Also, constraint (14b) is valid when the pump is in the on state. Therefore we replace the nonlinear pump head loss constraint in (2a) with its corresponding linear form (14b) while implementing big-*M* for the pump head loss, which is not shown here due to space limitations.

B. Dinkelbach's Transform for FSP Power

Attention is now turned to the nonlinear fractional FSP power consumption in (12). Substituting (1d) and (6) (when $x_{ij,t} = 1$) in (12), the FSP power is given as

$$p^{\text{pump}}_{ij,t}(q_{ij,t}, \eta^{\text{pump}}_{ij,t}) = \gamma_{ij}\frac{\left(h_{0,ij}q_{ij,t} - \sigma_{ij}q^{\nu_{ij}+1}_{ij,t}\right)}{a_{0,ij} + a_{1,ij}q_{ij,t} + a_{2,ij}q^2_{ij,t}},\ ij \in \mathcal{P} \tag{15}$$

Denote the numerator of (15) as $f_{ij,t}(q_{ij,t})$ and note that $(f_{ij,t}(q_{ij,t}))'' \leq 0$. Furthermore, from (7), we have that $a_{2,ij} < 0$. It follows that both the numerator and denominator of (15) are concave in the pump flows. Hence we devise linear upper bounds to both the numerator and the denominator of (15) as follows

$$\hat{f}_{ij,t}(q_{ij,t}, x_{ij,t}) = \left(\alpha_{ij,t}q_{ij,t} + \beta_{ij,t}x_{ij,t}\right) \tag{16a}$$

$$\hat{\eta}^{\text{pump},Q}_{ij,t}(q_{ij,t}) = \left(\alpha^1_{ij,t}q_{ij,t} + \beta^1_{ij,t}\right) \tag{16b}$$

where $\alpha_{ij,t}$, $\beta_{ij,t}$, $\alpha^1_{ij,t}$ and $\beta^1_{ij,t}$ are constants which are computed from the pump flows $\langle q_{ij,t}\rangle$ at the previous iteration so that the slopes and function values of (16) match their concave function counterparts at $\langle q_{ij,t}\rangle$.

Using (16), we express the nonlinear fractional pump power in (15) as linear fractional as follows

$$\hat{p}^{\text{pump}}_{ij,t}(q_{ij,t}, \hat{\eta}^{\text{pump},Q}_{ij,t}) = \gamma_{ij}\frac{\hat{f}_{ij,t}}{\hat{\eta}^{\text{pump},Q}_{ij,t}},\ ij \in \mathcal{P} \tag{17}$$

The FSP pump power approximation in (17) is still a fraction and hence nonconvex. Therefore, minimizing (17) is still computationally expensive. Note that $\hat{f}_{ij,t} > 0$ when pump is on ($x_{ij,t} = 1$); and $\hat{\eta}^{\text{pump},Q}_{ij,t} > 0$ when pump is on or off due to $a_{0,ij} > 0$. Therefore, Dinkelbach's transform [21] can be used to to reformulate (17) so that its numerator and denominator are decoupled. The main idea is to replace the fraction (17) with the difference between the numerator and denominator:

$$\tilde{\Gamma}^{\text{pump}}_{ij,t}(q_{ij,t}, \hat{\eta}^{\text{pump},Q}_{ij,t}) = \gamma_{ij}\left(\hat{f}_{ij,t} - \zeta_{ij,t}\hat{\eta}^{\text{pump},Q}_{ij,t}\right) \tag{18}$$

where $\tilde{\Gamma}^{\text{pump}}_{ij,t}$ denote the WDN objective in linear form, and ζ_{ij} is new auxiliary variable that is updated in a iterative fashion with iteration index l and given as follows

$$\langle\zeta_{ij,t}\rangle_{l+1} = \frac{\langle\hat{f}_{ij,t}\rangle_l}{\langle\hat{\eta}^{\text{pump},Q}_{ij,t}\rangle_l},\ ij \in \mathcal{P} \tag{19}$$

where $\langle\hat{f}_{ij,t}\rangle_l$ and $\langle\hat{\eta}^{\text{pump},Q}_{ij,t}\rangle_l$ are computed using pump flows $q_{ij,t}$ at the l-th iteration.

TABLE I: Vector variables to solve C-OWF problem

Notation	Description
$\mathbf{h}_t$	$(h_{j,t}), j \in \mathcal{M}$
$(\hat{\mathbf{h}}_t, \mathbf{q}_t)$	$(h_{ij,t}, q_{ij,t}), ij \in \mathcal{L}$
$(\mathbf{x}_t, \hat{\mathbf{f}}_t)$	$(x_{ij,t}, \hat{f}_{ij,t}), ij \in \mathcal{P}$
$(\mathbf{v}_t, \mathbf{r}_t)$	$(v_{ij,t}, r_{ij,t}), ij \in \mathcal{V}$
$\mathbf{d}_t$	$(d_{j,t}), j \in \mathcal{J}$
$\hat{\boldsymbol{\eta}}^{\text{pump},Q}_t$	$\hat{\eta}^{\text{pump},Q}_t, ij \in \mathcal{P}$
$\boldsymbol{\kappa}_t$	$(\kappa_{ij,t}), ij \in \mathcal{W}$
$(\boldsymbol{\tau}_t, \boldsymbol{\psi}_t, \boldsymbol{\alpha}_{ij,t}, \boldsymbol{\beta}_{ij,t})$	$(\tau_t, \psi_t, \alpha_{ij,t}, \beta_{ij,t}), ij \in \mathcal{P}$
$(\boldsymbol{\alpha}^1_{ij,t}, \boldsymbol{\beta}^1_{ij,t}, \boldsymbol{\vartheta}_{ij,t}, \boldsymbol{\epsilon}_{ij,t}, \boldsymbol{\zeta}_t)$	$(\alpha^1_{ij,t}, \beta^1_{ij,t}, \vartheta_{ij,t}, \epsilon_{ij,t}, \zeta_{ij,t}), ij \in \mathcal{P}$
$\mathbf{h}_0$	$(h_{k,0}), k \in \mathcal{K}$
$\mathbf{o}$	Operational limits of WDN (1e), (1i), (1j).
$\mathbf{y}_t$	A vector collecting $\mathbf{h}_t$, $\hat{\mathbf{h}}_t$, $\mathbf{x}_t$, $\mathbf{q}_t$, and $\mathbf{v}_t$.
$\hat{\mathbf{y}}_t$	A vector collecting $\boldsymbol{\kappa}_t$, $\boldsymbol{\tau}_t$, $\boldsymbol{\psi}_t$, $\boldsymbol{\alpha}_t$, $\boldsymbol{\beta}_t$, $\boldsymbol{\alpha}^1_{ij,t}$, $\boldsymbol{\beta}^1_{ij,t}$, $\boldsymbol{\vartheta}_{ij,t}$, $\boldsymbol{\epsilon}_{ij,t}$, and $\boldsymbol{\zeta}_t$.

Since (8) can also be shown to be concave in the flow, the cubic efficiency curve (8) is also upper-bounded by a linear function

$$\hat{\eta}^{\text{pump},C}_{ij,t}(q_{ij,t}) = \left(\vartheta_{ij,t}q_{ij,t} + \epsilon_{ij,t}\right) \tag{20}$$

To represent (15) with cubic efficiency, we replace $\hat{\eta}^{\text{pump},Q}_{ij,t}$ in (17), (18), and (19) with (20).

C. Convex-Optimal Water Flow Problem (C-OWF)

The previous transformations approximate all nonlinear constraints of WDNs (1b), (1d), and (1h) by linear ones. The parameters $\kappa_{ij,t}$, $\tau_{ij,t}$ and $\psi_{ij,t}, ij \in \mathcal{L}$ are all constants which are evaluated from the flow values of the previous iteration. The pipe and pump head loss approximations $\hat{h}_{ij,t},\ ij \in \mathcal{L}$ are all linear, but they are not equivalent to the first-order Taylor approximations.

The C-OWF problem (P2) can be stated as follows

$$\text{(P2)}\quad \min \quad \sum_{t=1}^{T}\left[\lambda_t \sum_{ij\in\mathcal{P}} \tilde{\Gamma}^{\text{pump}}_{ij,t}\right] \tag{21a}$$

$$\text{over} \quad \{q_{ij,t}, r_{ij,t}, \hat{f}_{ij,t}, \hat{\eta}^{\text{pump},Q}_{ij,t}\}^T_{t=1},\ \{\hat{h}_{ij,t}, h_{j,t}, x_{ij,t}, v_{ij,t}\}^T_{t=1},\ ij \in \mathcal{L}, j \in \mathcal{M}$$

$$\text{subj. to} \quad \text{(1a), (1c), (1i), (1j), (2), (3), (14), (16)} \tag{21b}$$

The C-OWF problem (P2) is a MILP problem. We use the term convex in C-OWF to emphasize that the continuous part of (21) is convex (in fact, linear). Modern mixed integer linear programming software can reliably solve instances of (21).

The objective is linear owning to the application of Dinkelbach's transform. Moreover, the decoupling of numerator and denominator of (17) can also be done using the classical Charnes-Cooper Transform while simultaneously introducing additional constraint; see, e.g., [27] for a detailed discussion. Also, it has been shown in [23] that for a fractional program with a single ratio as objective, Dinkelbach's transform has a fast convergence rate.

The C-OWF problem (21) is solved in an iterative fashion as summarized in Algorithm 1. The algorithm may result in oscillations in the error due to updates in the binary variables, i.e., the schedules of pumps and valves. Our numerical tests indicate that the binary variables remain the same after a number of iterations, after which the continuous variables may keep being updated but without oscillations.

The water utility operator implements the solution to the C-OWF problem. For notational convenience, we define the relevant vectors for WDNs in Table I.

Dinkelbach's algorithm is guaranteed to converge for fractional programs with a convex feasible set [21]. In the present case, the feasible set is nonconvex. The intuition is that after a few

Algorithm 1: C-OWF Iterative Algorithm

Input : Water utility operator acquires WDN topology, operational limits $\mathbf{o}$, tanks inital condition $\mathbf{h}_0$ and forecasted demands $\{\mathbf{d}_t\}_{t=1}^T$

Output: $\langle\{\mathbf{y}_t\}_{t=1}^T\rangle_{\text{final}}$

Initialize $l=0$ and $\langle\{\mathbf{y}_t\}_{t=1}^T\rangle_0$;

Set $\langle\{\mathbf{y}_t\}_{t=1}^T\rangle_{\text{save}} = \langle\{\mathbf{y}_t\}_{t=1}^T\rangle_0$, $l=1$, maxIter ;

while error $\geq$ tolerance *OR* $l \leq$ maxIter **do**

  Obtain $\langle\{\hat{\mathbf{y}}_t\}_{t=1}^T\rangle_l$ from $\langle\{\mathbf{y}_t\}_{t=1}^T\rangle_{\text{save}}$;

  Solve C-OWF problem (P2) over $\{\mathbf{q}_t, \mathbf{r}_t, \hat{\mathbf{f}}_t, \hat{\boldsymbol{\eta}}_t^{\text{pump},Q}, \mathbf{h}_t, \hat{\mathbf{h}}_t, \mathbf{x}_t, \mathbf{v}_t\}_{t=1}^T$; and set $\langle\{\mathbf{y}_t\}_{t=1}^T\rangle_l$ as its solution ;

  Calculate error := $\text{norm}(\langle\{\mathbf{y}_t\}_{t=1}^T\rangle_l - \langle\{\mathbf{y}_t\}_{t=1}^T\rangle_{\text{save}})$;

  Update $\langle\{\mathbf{y}_t\}_{t=1}^T\rangle_{\text{save}} = \langle\{\mathbf{y}_t\}_{t=1}^T\rangle_l$, and $l = l+1$

end

Set $\langle\{\mathbf{y}_t\}_{t=1}^T\rangle_l = \langle\{\mathbf{y}_t\}_{t=1}^T\rangle_{\text{final}}$;

Water utility operator communicate setpoints $\{\mathbf{x}_t, \mathbf{v}_t, \mathbf{r}_t\}_{t=1}^T$ to pumps and PRVs.

iterations of Algorithm 1, the binary variables do not change, and the coefficients of the linear approximations in (14) approximately converge, rendering the feasible set approximately linear. Indeed, we observe the expected behavior, that is, the left hand-side of (18) converges to zero and $\zeta_{ij,t}$ converges to the pump power (17).

VI. Numerical Results

This section examines the C-OWF solver's performance in terms of operating pumps near their maximum efficiency and by reducing pump power consumption in comparison to rule-based designs.

Network Setup: The present work considers the 10-node WDN depicted in Fig. 1. The system is operated over a time horizon of $T = 12$ hours, beginning at 8 AM with δ as one hour. The optimizations are solved using the MATLAB-based toolbox CVX along with the mixed-integer solver Gurobi [28]. All simulations are run on a 3.60-GHz, intel core i7 computer with 32 GB of RAM. For WDNs, the head unit is feet [ft]; and the flow unit is gallons per minute [GPM]. Fig. 2 illustrates the network-wide water demand, which is chosen to reflect reasonable conditions.

The pipe lengths, diameters, node elevations, tank diameter, and junction base demands are obtained from the 8-node WDN [15] wherein two additional nodes with one PRV are added. The bounds on pump flows are $[f_{\min}, f_{\max}]$ = [0, 2400] GPM. The tank minimum height, maximum height, and initial level are respectively set to $h_{\min} = 830$ ft, $h_{\max} = 850$ ft, and $h_0 = 840$ ft. Furthermore, we consider an FSP with parameters $h_0 = 266.67$ ft, $\sigma = 4.629 \times 10^{-5}$, and $\nu = 2$ computed from EPANET [15]. The pump best operating point, i.e., (q_{ij}^*, η_{ij}^*) is chosen as $[1200, 0.9]$, and the cutoff flow of the pump $\tilde{q}_{ij}$ is 2400 GPM computed by the EPANET. The previously mentioned values are used to compute the coefficients of the pump efficiency curve in (6) and (8) as described in Section II. Moreover, the coefficient $a_{0,ij}$ in (6) and (8) is assumed to be 0.00001. Three test cases, I through III, are considered. The parameters in the Algorithm 1 are selected as tolerance $= 0.001$ and maxIter $= 400$ for Test Cases II and III. The value of λ_t in (P2) is chosen to be 1 for all test cases.

Test Case I: EPANET's rule-based controls are used to modify the controllable elements' status based on the safe water level in tanks. The pump efficiency curve (quadratic/cubic) in EPANET only allows for computing pump power and does not guarantee operation of the pump at the best efficiency point [15, Ch. 3]. This is a base case against which C-OWF is compared, as EPANET's rule-based controls is one of the most prevalent methods for pump scheduling accounting for efficiency curves.

Test Case II: In this test case we solve problem (P2) assuming constant pump efficiency, $\eta_{ij}^{\text{pump}} = 0.9$. Upon solving (P2), we first use pump flows to compute pump efficiencies from (6) (quadratic) and (8) (cubic). The pump power is then computed using pump flows, pump heads, and the pump efficiency from (15). This test case shows that assuming constant pump efficiency in the optimization (as is typical in much of the literature) does not guarantee pump operation close to the best efficiency point.

Test Case III: We first solve problem (P2) using Algorithm 1 considering flow-dependent pump efficiency given by (16b) (for quadratic curve) and (20) (for cubic curve). Second, following similar approach as in Test Case II, we evaluate the pump efficiency and pump power using (6), (8), and, (15).

Although we use linear approximations to solve Test Cases II and III, we utilize the exact nonlinear solver EPANET to evaluate the feasibility and modeling accuracy of the C-OWF solver.

Table II compares the pump power and pump efficiency values for all test cases. It is evident from Table II that Test Case III achieves lower pump power consumption under both quadratic and cubic efficiencies when compared to Test Case II and I. This is because the pumps are operated close to their best efficiency point in Test Case III. Moreover, the pump efficiency attains its maximum value using cubic efficiency in Test Case III, i.e., 90%. Therefore, Test Case III achieved an actual reduction in pump power compared to Test Cases I and II. For example, the pump power in Test Case III with cubic efficiency is respectively reduced by 2.25% and 1.2% compared to Test Cases I and II. Since the reduction values are based on a 12-hour operation, the savings should eventually be assessed over a sufficiently long period (e.g., annually).

Furthermore, it can be seen from Table II that Test Case III maintains pump efficiency close to maximum. For example, with cubic efficiency, the pump's minimum efficiency is 86.87% in Test Case I and 88.97% in Test Case II. In contrast, the minimum efficiency of the pump is 89.41% in Test Case III. Also, the pump's average efficiency in Test Case III is higher compared to Test Case I and II. These results indicate that including the flow-dependent pump efficiency in the optimization allows the pump to operate close to its best efficiency point and at the same time leads to a significant % reduction in pump power.

Table III lists the pump on/off status for different test cases. The results for Test Case III in Table III are presented for quadratic and cubic efficiency. Although the on/off schedules of Test Case III with quadratic and cubic efficiencies are similar, we observed that the total pump flows for cubic efficiency are less than with quadratic efficiency. Similarly, the total pump flows for Test Case III are less when compared to Test Case I and II. Considering the flow-dependent efficiency in the objective implicitly results in the pump to operating close to its best efficiency point and contributes to water conservation.

The computational time for Test Cases II and III is less than 2 minutes. Finally, the modeling accuracy of the developed linearizations, that is, the flows, heads, and pump power consumption computed using C-OWF solver, is compared with the benchmark software EPANET, which uses the nonlinear hydraulics. For the present case study, the nodal heads and flows found by the two models differ at most by 0.001 ft and 0.02 GPM, respectively. The pump power computed by the two models differs by 0.05 kW.

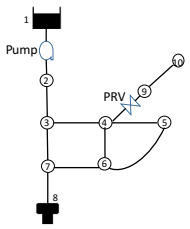

Fig. 1: 10-node WDN with one pump, one PRV, and one tank for the test cases considered.

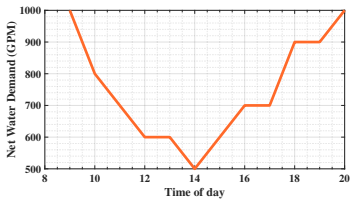

Fig. 2: Network-wide water demand profile.

VII. Conclusions

This work develops a solver (C-OWF) to solve nonconvex OWF problems considering flow-dependent pump efficiency. The merits of the proposed approach are demonstrated in terms of pump power reduction and energy-efficient operation of WDNs for the pilot study of this work. Future work will look at incorporating the variable-speed pumps (VSPs) along with flow and speed-dependent VSP efficiency using convex optimization approaches. Future work will also experiment with larger WDNs and more formally investigate the algorithm convergence. Future work will also examine methods for incorporating water demand uncertainty into the developed solver.

TABLE II: Test Case comparisons

Test Case	Test Case I		Test Case II		Test Case III	
	quad eff.	cubic eff.	quad eff.	cubic eff.	quad eff.	cubic eff.
$\sum_t \sum_{ij\in\mathcal{P}} P^{\text{pump}}_{ij,t}$ (kW)	233.58	233.14	230	229.31	228.19	227.90
max $(\eta^{\text{pump}}_{ij,t})$ (%)	89.05	89.20	89.78	89.84	89.94	90
min $(\eta^{\text{pump}}_{ij,t})$ (%)	86.65	86.87	88.83	88.97	89.20	89.41
Avg. $(\eta^{\text{pump}}_{ij,t})$ (%)	88.10	88.27	89.29	89.39	89.53	89.61

TABLE III: Pump on/off comparisons

Test Case	1	2	3	4	5	6	7	8	9	10	11	12
Test Case I	0	0	0	0	0	0	0	1	1	0	1	1
Test Case II	0	1	0	1	0	0	0	1	1	0	0	0
Test Case III (quad eff.)	0	0	0	1	0	1	0	1	1	0	0	0
Test Case III (cubic eff.)	0	0	0	1	0	1	0	1	1	0	0	0

References

[1] "United nations, world population prospects: The 2015 revision, data booklet," Department of Economic and Social Affairs, Population Division, New York, USA, Tech. Rep., 2015.

[2] D. Denig-Chakroff, "Reducing electricity used for water production: Questions state commissions should ask regulated utilities," National Regulatory Research Institute, Washington, DC, Tech. Rep., Jun. 2008.

[3] B. Griffiths-sattenspiel and W. Wilson, "The carbon footprint of water," https://www.rivernetwork.org/resource/the-carbon-footprint-of-water, 2009.

[4] A. Marchi, A. Simpson, and N. Ertugrul, "Assessing variable speed pump efficiency in water distribution systems," *Drinking Water Engineering and Science Discussions*, vol. 5, Mar. 2012.

[5] B. T. Abe, P. Shrivastava, and K. Moloi, "A review of energy consumption in water supply systems," in *Proc. (IEEE) AFRICON*, Accra, Ghana, Ghana, Sep. 2019, pp. 1–4.

[6] E. Cabrera, M. A. Pardo, R. Cobacho, and E. Cabrera, "Energy audit of water networks," *J. Water Resour. Planning and Manag.*, vol. 136, no. 6, pp. 669–677, 2010.

[7] E. Dall'Anese, P. Mancarella, and A. Monti, "Unlocking flexibility: Integrated optimization and control of multienergy systems," *IEEE Power Energy Mag.*, vol. 15, no. 1, pp. 43–52, Jan. 2017.

[8] X. Zhang and V. V. Vesselinov, "Energy-water nexus: Balancing the tradeoffs between two-level decision makers," *Appl. Energy*, vol. 183, pp. 77 – 87, Dec. 2016.

[9] A. M. Gleixner, H. Held, W. Huang, and S. Vigerske, "Towards globally optimal operation of water supply networks," *Numerical Algebra, Control & Optim.*, vol. 2, pp. 695–711, 2012.

[10] R. Menke, E. Abraham, P. Parpas, and I. Stoianov, "Exploring Optimal Pump Scheduling in Water Distribution Networks with Branch and Bound Methods," *Water Resour. Manag.*, vol. 30, no. 14, pp. 5333–5349, Oct. 2016.

[11] D. Verleye and E.-H. Aghezzaf, "Optimising production and distribution operations in large water supply networks: A piecewise linear optimisation approach," *Int. J. Production Res.*, vol. 51, no. 23-24, pp. 7170–7189, 2013.

[12] B. Ghaddar, J. Naoum-Sawaya, A. Kishimoto, N. Taheri, and B. Eck, "A lagrangian decomposition approach for the pump scheduling problem in water networks," *Eur. J. Oper. Res.*, vol. 241, no. 2, pp. 490 – 501, Mar. 2015.

[13] M. K. Singh and V. Kekatos, "Optimal scheduling of water distribution systems," *IEEE Trans. Control Netw. Syst.*, pp. 1–1, 2019, early access.

[14] D. Fooladivanda and J. A. Taylor, "Energy-optimal pump scheduling and water flow," *IEEE Trans. Control Netw. Syst.*, vol. 5, no. 3, pp. 1016–1026, Feb. 2017.

[15] L. A. Rossman, "Epanet 2 user's manual," Environmental Protection Agency, Washington, DC, USA, Tech. Rep., Nov. 2000.

[16] A. Martin-Candilejo, D. Santillán, and L. Garrote, "Pump efficiency analysis for proper energy assessment in optimization of water supply systems," *Water*, vol. 12, no. 1, p. 132, 2020.

[17] Y. Wang, V. Puig, and G. Cembrano, "Non-linear economic model predictive control of water distribution networks," *Journal of Process Control*, vol. 56, pp. 23–34, 08 2017.

[18] S. Wang, A. F. Taha, L. Sela, M. H. Giacomoni, and N. Gatsis, "A new derivative-free linear approximation for solving the network water flow problem with convergence guarantees," *Water Resour. Res.*, vol. 56, no. 3, p. e2019WR025694, Jan. 2020.

[19] S. Wang, A. Taha, N. Gatsis, and M. Giacomoni, "Receding horizon control for drinking water networks: The case for geometric programming," *IEEE Trans. Control Netw. Syst.*, pp. 1–1, 2020, early access.

[20] S. Wang, A. F. Taha, L. Sela, N. Gatsis, and M. H. Giacomoni, "State estimation in water distribution networks through a new successive linear approximation," in *Proc. (IEEE) Conf. Decis. Control (CDC)*, Nice, France, Dec. 2019, pp. 5474–5479.

[21] W. Dinkelbach, "On nonlinear fractional programming," *Management Science*, vol. 13, no. 7, pp. 492–498, 1967.

[22] Y. Gao and S. Jin, "A Global Optimization Algorithm for Sum of Linear Ratios Problem," *Journal of Applied Mathematics*, vol. 2013, p. 276245, 2013.

[23] K. Shen and W. Yu, "Fractional programming for communication systems—part I: Power control and beamforming," *IEEE Trans. Signal Process.*, vol. 66, no. 10, pp. 2616–2630, 2018.

[24] Y. Amerlinck, I. Hitsov, D. Gaublomme, and I. Nopens, "A decision support system for design of a water treatment facility - functional analysis report," Tech. Rep., Sep. 2019.

[25] B. Ulanicki, J. Kahler, and B. Coulbeck, "Modeling the efficiency and power characteristics of a pump group," *J. Water Resour. Plan. Man.-ASCE*, vol. 134, pp. 88–93, Jan. 2008.

[26] T. M. Walski, D. V. Chase, D. A. Savic, W. Grayman, S. Beckwith, and E. Koelle, *Advanced Water Distribution Modeling and Management*. Civil and Environmental Engineering and Engineering Mechanics Faculty Publications, 2013.

[27] A. Charnes and W. W. Cooper, "Programming with linear fractional functionals," *Naval Research Logistics Quarterly*, vol. 9, no. 3-4, pp. 181–186, 1962.

[28] M. Grant and S. Boyd, "CVX: Matlab software for disciplined convex programming, version 2.1," http://cvxr.com/cvx, Mar. 2014.